Mathematical Biosciences and Engineering

http://www.aimspress.com/journal/mbe

MBE, 21(4): 5499–5520.
DOI: 10.3934/mbe.2024242
Received: 21 December 2023
Revised: 03 February 2024
Accepted: 19 February 2024
Published: 19 March 2024

Research article

Dynamical analysis of a discrete two-patch model with the Allee effect and nonlinear dispersal

Minjuan Gao, Lijuan Chen*and Fengde Chen

School of Mathematics and Statistics, Fuzhou University, Fuzhou 350108, Fujian, China

* **Correspondence:** E-mail: chenlijuan@fzu.edu.cn.

Abstract: The dynamic behavior of a discrete-time two-patch model with the Allee effect and nonlinear dispersal is studied in this paper. The model consists of two patches connected by the dispersal of individuals. Each patch has its own carrying capacity and intraspecific competition, and the growth rate of one patch exhibits the Allee effect. The existence and stability of the fixed points for the model are explored. Then, utilizing the central manifold theorem and bifurcation theory, fold and flip bifurcations are investigated. Finally, numerical simulations are conducted to explore how the Allee effect and nonlinear dispersal affect the dynamics of the system.

Keywords: flip bifurcation; fold bifurcation; Allee effect; nonlinear dispersal

1. Introduction

The Allee effect [1] refers to a phenomenon in population biology where the fitness and survival rates of individuals decrease when the population size becomes smaller. It suggests that certain species require a minimal population size to effectively find mates, protect against predation, or efficiently gather resources such as food. When the density of a population falls below this critical threshold, reproductive success and overall survival can be hindered (see [2–4] and the references cited therein).

In recent years, there has been increasing interest in studying the dynamics of patchy populations, where habitats are separated by unsuitable areas. The movement of individuals between patches, known as dispersal, is an important factor in determining the persistence and stability of such populations. Researchers have begun to study the dynamics of two-patch models with strong Allee effect [5]. These studies have revealed some interesting behaviors that were not previously understood [6–8]. Recently, Kang et al. [9] studied the following two-patch model with strong Allee effect:

$$\begin{aligned} \frac{du}{dt} &= ru(1-u)(u-\theta) + D(v-u), \\ \frac{dv}{dt} &= rv(1-v)(v-\theta) + D(u-v), \end{aligned}$$

where $D \in [0, 1]$ is the dispersal parameter, representing the fraction of population migration from one patch to the other per unit of time.

In [10], the authors proposed the following one species model with additive Allee effect and dispersal:

$$\begin{aligned} \frac{du}{dt} &= -u + D_2 v - D_1 u, \\ \frac{dv}{dt} &= v(1 - v - \frac{m}{v + a}) + D_1 u - D_2 v. \end{aligned}$$

The results indicate that when the Allee effect constant a increases or m decreases, the total population abundance increases. In addition, when the dispersal rate D_1 increases or D_2 decreases, the total population density increases. An additive Allee effect can deduce complex dynamics such as saddle-nodes and transcritical bifurcations.

In [11], the author proposed the following model with linear dispersal:

$$\frac{du^j}{dt} = u^j(a^j - b^j u) + \sum_{k=1}^{m} D(u^k - u^j),\ j = 1, ..., m,$$

where D is the dispersal constant. Later, Allen [11] pointed out that the diffusion rate may be influenced by population density and proposed a patchy model with biased (nonlinear) diffusion as follows:

$$\frac{du^j}{dt} = u^j(a^j - b^j u) + \sum_{k=1}^{m} Du^j(u^k - u^j),\ j = 1, ..., m.$$

As is also shown in [12, 13], populations might disperse non-linearly in complex real-life environments. Recently, Xia et al. [14] studied the following two-patch model with Allee effect and nonlinear dispersal:

$$\begin{cases} \frac{du}{dt} = u(\frac{ru}{A+u} - d - bu) + Du(v - u), \\ \frac{dv}{dt} = v(a - cv) + Dv(u - v), \end{cases} \tag{1.1}$$

where u, v are the densities of the population in the first patch and the second patch, respectively. A is the Allee effect constant. r, d, and b are the birth rate, natural mortality, and death rate due to intra-prey competition in the first patch, respectively. a and c are the intrinsic growth rate and the death rate due to intra-prey competition of population in the second patch, respectively. D is the dispersal coefficient.

It is well known that discrete models defined by difference equations are preferable to continuous-time ones when a species has non-overlapping generations or a limited population size. Recently, in [15, 16], the authors studied discrete-time systems with Allee effects. In [17, 18], the authors investigated the effect of dispersal on asymptotic total population size in the discrete two-patch model. However, to the best of the authors' knowledge, up to now a discrete two-patch model incorporating the Allee effect and nonlinear dispersal has never been put forth. Motivated by the above and with the assistance of the piecewise constant parameter method introduced by Jiang and Rogers [19], we convert model (1.1) into a discrete one as follows:

$$\begin{cases} \frac{du}{u(t)dt} = \frac{ru([t])}{A+u([t])} - d - bu([t]) + D(v([t]) - u([t])), \\ \frac{dv}{v(t)dt} = a - cv([t]) + D(u([t]) - v([t])), \end{cases} \tag{1.2}$$

where $0 \le n \le t < n+1$ and $[t]$ is the greatest integer less than or equal to t. Since the right hand side of system (1.2) is constant over the interval $[n, n+1)$, integrating over $[n, t)$ and letting $t \to n+1$, it yields

$$\begin{cases} \ln \frac{u(n+1)}{u(n)} = \frac{ru(n)}{A+u(n)} - d - bu(n) + D(v(n) - u(n)), \\ \ln \frac{v(n+1)}{v(n)} = a - cv(n) + D(u(n) - v(n)). \end{cases} \tag{1.3}$$

Denoting $u(n)$ by u_n and $v(n)$ by v_n, we thus obtain the following discrete-time model:

$$\begin{cases} u_{n+1} = u_n \exp(\frac{ru_n}{A+u_n} - d - bu_n + D(v_n - u_n)), \\ v_{n+1} = v_n \exp(a - cv_n + D(u_n - v_n)). \end{cases} \tag{1.4}$$

Different from the continuous two-patch model (1.1) in Xia et al. [14], this is the first time that the discrete two-patch model with nonlinear dispersal and the Allee effect has been proposed. The corresponding dynamic behaviors will be investigated in detail. We will also conclude that immediate nonlinear dispersal other than large nonlinear dispersal in [14] will be more conducive to the survival of the species.

The rest of the paper is organized as follows. In Section 2, we discuss the existence and stability of fixed points of system (1.4). In Section 3, we present the complete analysis of bifurcation. The influence of the Allee effect and nonlinear dispersal is presented in Section 4. A brief summary and discussion is in Section 5.

2. Existence and stability of fixed points of (1.4)

To obtain the fixed point of (1.4), we need to solve the following equation:

$$\begin{cases} u = u \exp\left(\frac{ru}{A+u} - d - bu + D(v - u)\right), \\ v = v \exp\left(a - cv + D(u - v)\right). \end{cases} \tag{2.1}$$

Clearly, (1.4) always has the boundary fixed points $E_0(0,0), E_{01}(0, \frac{a}{c+D})$. Moreover, the fixed point $E(u^*, 0)$ on the u coordinate axis exists where u^* satisfies the following equation:

$$F(u) := (b+D)u^2 + (d + bA + DA - r)u + dA = 0.$$

If $d + bA + DA - r \ge 0$, then system (1.4) has no other equilibrium on the coordinate axis. In the following we investigate the case $d + bA + DA - r < 0$, that is, $r > d + bA + DA$. Notice that the discriminant of $F(u)$ is $\Delta = (b+D)^2A^2 - 2(d+r)(b+D)A + (d-r)^2$. If $\Delta > 0$, then system (1.4) has two boundary fixed points $E_{10}(u_1^*, 0)$ and $E_{20}(u_2^*, 0)$, where u_1^* and u_2^* are the positive roots of the equation $F(u) = 0$. If $\Delta = 0$, then system (1.4) has a boundary fixed point $E_{30}(u_3^*, 0)$. In order to simplify the analysis, let

$$A_1 = \frac{d+r-2\sqrt{dr}}{b+D}, A^* = \frac{r-d}{b+D}.$$

Also, we have

$$\Delta \begin{cases} > 0 & \text{if } 0 < A < A_1, \\ = 0 & \text{if } A = A_1, \\ < 0 & \text{if } A_1 < A < A^*. \end{cases}$$

Theorem 2.1 System (1.4) always has two boundary fixed points, i.e., $E_0(0,0)$ and $E_{01}(0,\frac{a}{c+D})$. Moreover,

(1) if $r \le d + bA + DA$, then system (1.4) has no other boundary fixed point.

(2) if $r > d + bA + DA$, then

(i) system (1.4) also has two boundary fixed points $E_{10}(u_1^*,0)$ and $E_{20}(u_2^*,0)$ if $0 < A < A_1$, where $u_1^* = \frac{-(b+D)A-d+r-\sqrt{\Delta}}{2(b+D)}, u_2^* = \frac{-(b+D)A-d+r+\sqrt{\Delta}}{2(b+D)}$;

(ii) system (1.4) also has a boundary fixed point $E_{30}(u_3^*,0)$ if $A = A_1$, where $u_3^* = \frac{-d+\sqrt{dr}}{b+D}$;

(iii) system (1.4) has no other boundary fixed point if $A > A_1$.

A positive fixed point (u,v) of system (1.4) satisfies

$$\begin{cases} \frac{ru}{A+u} - d - bu + D(v-u) = 0, \\ a - cv + D(u-v) = 0, \end{cases} \tag{2.2}$$

that is,

$$\left(b + \frac{cD}{c+D}\right)u^2 + \left(Ab + \frac{cDA}{c+D} + d - \frac{aD}{c+D} - r\right)u + \left(d - \frac{aD}{c+D}\right)A = 0. \tag{2.3}$$

To simplify the analysis, let

$$m := b + \tfrac{cD}{c+D},\ n := d - d^{**},\ d^{**} := \tfrac{aD}{c+D},$$

Equation (2.3) becomes

$$mu^2 + (Am + n - r)u + nA = 0. \tag{2.4}$$

Notice that the discriminant of (2.4) is $\Delta_1(m) = (Am + n - r)^2 - 4mnA = (Am - n - r)^2 - 4nr$.

If $d = d^{**}$, Equation (2.4) becomes

$$mu^2 + (Am - r)u = 0. \tag{2.5}$$

Therefore, if $r \le mA$, there is no positive equilibrium; if $r > mA$, Equation (2.5) has a unique positive real root.

If $0 < d < d^{**}$, Equation (2.4) has a unique positive real root.

If $d \ge d^{**} + r$, i.e., $n \ge r$, Equation (2.4) has no positive real root.

In the following, we investigate the case $d^{**} < d < d^{**} + r$. If $m \ge \frac{r-n}{A}$, Equation (2.4) has no positive real root. Next, we consider the case $m < \frac{r-n}{A}$. The discriminant of $\Delta_1(m)$ is $\Delta_2 = 16nrA^2 > 0$. Thus, $\Delta_1(m) = 0$ has two positive real roots, i.e.,

$$m_1 = \tfrac{(\sqrt{n}-\sqrt{r})^2}{A},\ m_2 = \tfrac{(\sqrt{n}+\sqrt{r})^2}{A}.$$

We get $m_1 < \frac{r-n}{A} < \frac{r+n}{A} < m_2$. Therefore, if $m = m_1$, Equation (2.4) has a unique positive real root. If $m < m_1$, Equation (2.4) has two positive real roots. If $m > m_1$, it follows that $\Delta_1(m) < 0$ and then Eq (2.4) has no positive real root. Thus, we have the existence of a positive fixed point as follows:

Theorem 2.2

(1) If $0 < d < d^{**}$, then system (1.4) has a positive fixed point $E_1^*(u_1, v_1)$.

(2) If $d = d^{**}$, then

(i) system (1.4) has a positive fixed point $E_1^*(u_1, v_1)$ when $r > mA$;

(ii) system (1.4) has no positive fixed point when $r \le mA$.

(3) If $d^{**} < d < d^{**} + r$, then

(i) system (1.4) has two positive fixed points $E_1^*(u_1, v_1)$ and $E_2^*(u_2, v_2)$ when $m < m_1$;

(ii) system (1.4) has a positive fixed point $E_3^*(u_3, v_3)$ when $m = m_1$;

(iii) system (1.4) has no positive fixed point when $m > m_1$.

(4) If $d \ge d^{**} + r$, then system (1.4) has no positive fixed point.

And,

$$\begin{aligned} u_1 &= \tfrac{-Am-n+r+\sqrt{\Delta_1(m)}}{2m}, \quad v_1 = \tfrac{Du_1+a}{c+D} = \tfrac{2am+D(r-Am-n)+D\sqrt{\Delta_1(m)}}{2m(c+D)}, \\ u_2 &= \tfrac{-Am-n+r-\sqrt{\Delta_1(m)}}{2m}, \quad v_2 = \tfrac{Du_2+a}{c+D} = \tfrac{2am+D(r-Am-n)-D\sqrt{\Delta_1(m)}}{2m(c+D)}, \\ u_3 &= \tfrac{-Am-n+r}{2m}, \quad v_3 = \tfrac{Du_1+a}{c+D} = \tfrac{2am+D(r-Am-n)+D}{2m(c+D)}. \end{aligned}$$

Next, we will consider the local stability of the fixed point. The Jacobian matrix of system (1.4) at the equilibrium $E(u, v)$ is

$$J(E) = \begin{pmatrix} \left(1 + u(\frac{r}{A+u} - \frac{ru}{(A+u)^2} - b - D)\right)N & uDN \\ vDG & G - v(c+D)G \end{pmatrix},$$

where $N = \exp\left(\frac{ru}{A+u} - d - bu + D(v-u)\right)$ and $G = \exp\left(a - cv + D(u-v)\right)$. Let λ_1 and λ_2 be the two eigenvalues of $J(E)$. To study the local stability of these fixed points, we will use the classification definition of fixed points in [20] and obtain the following results:

Theorem 2.3 $E_0(0, 0)$ is always a saddle.

Proof. At the trivial fixed point $E_0(0, 0)$, the Jacobian matrix is

$$J(E_0) = \begin{pmatrix} e^{-d} & 0 \\ 0 & e^{a} \end{pmatrix}$$

with eigenvalues $\lambda_1 = e^{-d} \in (0, 1)$ and $\lambda_2 = e^a > 1$. Hence, $E_0(0, 0)$ is always a saddle.

Theorem 2.4 For $E_{01}(0, \frac{a}{c+D})$,

(1) it is a sink if and only if $0 < a < \min\{2, \frac{d(c+D)}{D}\}$;

(2) it is a source if and only if $a > \max\{2, \frac{d(c+D)}{D}\}$;

(3) it is non-hyperbolic if either $a = 2$ or $a = \frac{d(c+D)}{D}$;

(4) it is a saddle, except for in cases (1)–(3).

Proof. At the boundary fixed point $E_{01}(0, \frac{a}{c+D})$, the Jacobian matrix is

$$J(E_{01}) = \begin{pmatrix} e^{\frac{aD}{c+D}-d} & 0 \\ \frac{aD}{c+D} & 1-a \end{pmatrix}$$

with eigenvalues $\lambda_1 = e^{\frac{aD}{c+D}-d}$ and $\lambda_2 = 1 - a$. It is easy to see that

$$1-a\begin{cases}<-1 & \text{if } a>2,\\ =-1 & \text{if } a=2,\\ \in(-1,1) & \text{if } 0<a<2\end{cases}$$

and

$$e^{\frac{aD}{c+D}-d}\begin{cases}>1 & \text{if } a>\frac{d(c+D)}{D},\\ =1 & \text{if } a=\frac{d(c+D)}{D},\\ \in(-1,1) & \text{if } 0<a<\frac{d(c+D)}{D}.\end{cases}$$

Hence, the result is proved.

Theorem 2.5 The boundary fixed point $E_{30}(u_3^*, 0)$ is a non-hyperbolic.

Proof. At the boundary fixed point $E_{30}(u_3^*, 0)$, the Jacobian matrix is

$$J(E_{30}) = \begin{pmatrix} 1 & \frac{(\sqrt{dr}-d)D}{b+D} \\ 0 & e^{a+\frac{(\sqrt{dr}-d)D}{b+D}} \end{pmatrix},$$

with eigenvalues $\lambda_1 = 1$ and $\lambda_2 = e^{a+\frac{(\sqrt{dr}-d)D}{b+D}} > 1$. Hence, the proof is complete.

Theorem 2.6 For the equilibrium $E_{i0}(u_i^*, 0)(i = 1, 2)$,

(1) it is a source if and only if $\frac{rA}{(A+u_i^*)^2} > b + D$;

(2) it is non-hyperbolic if and only if $\frac{rA}{(A+u_i^*)^2} = b + D$;

(3) it is a saddle if and only if $b + D - 2 < \frac{rA}{(A+u_i^*)^2} < b + D$.

Proof. At the boundary fixed point $E_{i0}(u_i^*, 0), (i = 1, 2)$, the Jacobian matrix is

$$J(E_{i0}(u_i^*, 0)) = \begin{pmatrix} 1 + u_i^*(\frac{r}{A+u_i^*} - \frac{ru_i^*}{(A+u_i^*)^2} - M) & u_i^* D \\ 0 & e^{a+u_i^* D} \end{pmatrix}.$$

The corresponding eigenvalues are $\lambda_1 = 1 + u_i^*(\frac{r}{A+u_i^*} - \frac{ru_i^*}{(A+u_i^*)^2} - b - D)$ and $\lambda_2 = e^{a+u_i^* D} > 1$. When $b + D > 2$, it is easy to see that

$$|\lambda_1|\begin{cases}>1 & \text{if } \frac{rA}{(A+u_i^*)^2} > b + D,\\ =1 & \text{if } \frac{rA}{(A+u_i^*)^2} = b + D,\\ <1 & \text{if } b + D - 2 < \frac{rA}{(A+u_i^*)^2} < b + D.\end{cases}$$

Hence, the proof is complete.

Theorem 2.7 If $\frac{r}{A} < b$, then the positive fixed point $E^*(u_*, v_*)$ is

(1) a sink if and only if $P < 1 + Q$ *and* $Q < 1$;

(2) a source if and only if $P < 1 + Q$ *and* $Q > 1$;

(3) non-hyperbolic if and only if $P = 1 + Q$;

(4) a saddle if and only if $P > 1 + Q$, *where*

Table 1. Feasibility and local stability criteria of the fixed points of system (1.4).

Fixed point	Feasibility conditions	Stability criteria
$E_0(0,0)$	always feasible	saddle
$E_{01}(0, \frac{a}{c+D})$	always feasible	$0 < a < \min\{2, \frac{d(c+D)}{D}\}$, sink $a > \max\{2, \frac{d(c+D)}{D}\}$, source $a = 2$ or $a = \frac{d(c+D)}{D}$, non-hyperbolic others, saddle
$E_{10}(u_1^*, 0)$, $E_{20}(u_2^*, 0)$	$r > d + bA + DA$, $0 < A < A_1$	$\frac{rA}{(A+u_i^*)^2} > b + D$, source $\frac{rA}{(A+u_i^*)^2} = b + D$, non-hyperbolic $b + D - 2 < \frac{rA}{(A+u_i^*)^2} < b + D$, saddle
$E_{30}(u_3^*, 0)$	$r > d + bA + DA$, $A = A_1$	non-hyperbolic
$E_1^*(u_1, v_1)$	$0 < d < d^{**}$ or $d = d^{**}$, $r > mA$ or $d^{**} < d < d^{**} + r$, $m < m_1$	$P < 1 + Q$ and $Q < 1$, sink $P < 1 + Q$ and $Q > 1$, source $P = 1 + Q$, non-hyperbolic $P > 1 + Q$, saddle
$E_2^*(u_2, v_2)$	$d^{**} < d < d^{**} + r$, $m < m_1$	
$E_3^*(u_3, v_3)$	$d^{**} < d < d^{**} + r$, $m = m_1$	

$$P = -2 - u_*\left(\frac{rA}{(A+u_*)^2} - b - D\right) + a + Du_*,$$
$$Q = \left(1 + u_*\left(\frac{rA}{(A+u_*)^2} - b - D\right)\right)(1 - a - Du_*) - u_*v_*D^2.$$

Proof. At the positive fixed point $E^*(u_*, v_*)$, the Jacobian matrix is

$$J(E^*) = \begin{pmatrix} 1 + u_*\left(\frac{rA}{(A+u_*)^2} - b - D\right) & u_*D \\ v_*D & 1 - (c+D)v_* \end{pmatrix}.$$

The characteristic equation for $J(E^*)$ is $F(\lambda) = \lambda^2 + P\lambda + Q = 0$.

Thus,

$$\begin{aligned} F(1) &= 1 + P + Q \\ &= -u_*\left(\left(\frac{rA}{(A+u_*)^2} - b - D\right)(a + Du_*) + v_*D^2\right), \\ F(-1) &= 1 - P + Q. \end{aligned}$$

If $\frac{r}{A} < b$ holds, then $\frac{rA}{(A+u_*)^2} < \frac{r}{A} < b$ and $\frac{v_*D^2}{a+Du_*} = \frac{D^2}{c+D} < D$, implying that $F(1) > 0$. If the conditions $P < 1 + Q$ and $Q < 1$ hold, then $F(-1) > 0$, $Q < 1$. Hence, according to Lemmas 1 and 2 in [21], we obtain that $E^*(u_*, v_*)$ is a sink, which is stable. Cases (2)–(4) can be proved in the same way. Hence, Theorem 2.7 is obtained.

The feasibility and local stability criteria of the fixed points of system (1.4) are given in Table 1.

3. Bifurcation analysis

In the following, we will use the central manifold and bifurcation theories [22, 23] to discuss bifurcation in system (1.4). In detail, we will analyze the existence of a flip bifurcation at the fixed point $E_{01}(0, \frac{a}{c+D})$ and a fold bifurcation at the fixed points $E_{30}(u_3^*, 0)$ and $E_3^*(u_3, v_3)$.

Theorem 3.1 System (1.4) undergoes a flip bifurcation at $E_{01}(0, \frac{a}{c+D})$ when the parameters are varied in a small range of $F_A = \left\{(a, r, d, D, c) : a = 2, a \neq \frac{d(c+D)}{D}, r > 0, d > 0, D > 0, c > 0\right\}$.

Proof. Theorem 2.4(3) shows that if $a = 2$ and $a \neq \frac{d(c+D)}{D}$, then one of the eigenvalues of the fixed point $E_{01}(0, \frac{a}{c+D})$ is -1, and the other eigenvalue is neither 1 nor -1. Regarding a as the bifurcation parameter and perturbing a by ζ, system (1.4) can be seen as the two-dimensional map below:

$$\begin{pmatrix} u \\ v \end{pmatrix} \to \begin{pmatrix} u\exp(\frac{ru}{A+u} - d - bu + D(v-u)) \\ v\exp\left(a + \zeta - cv + D(u-v)\right) \end{pmatrix}, \tag{3.1}$$

where $|\zeta| \ll 1$. By allowing $x_1 = u, y_1 = v - \frac{a}{c+D}$, we then transform the fixed point $E_{01}(0, \frac{a}{c+D})$ of the system (1.4) into the origin and shift model (3.1) into

$$\begin{pmatrix} x_1 \\ \zeta \\ y_1 \end{pmatrix} \to \begin{pmatrix} e^{\frac{2D}{c+D}-d} & 0 & 0 \\ 0 & 1 & 0 \\ \frac{2D}{c+D} & \frac{2}{c+D} & -1 \end{pmatrix} \begin{pmatrix} x_1 \\ \zeta \\ y_1 \end{pmatrix} + \begin{pmatrix} f_1(x_1, \zeta, y_1) \\ 0 \\ g_1(x_1, \zeta, y_1) \end{pmatrix}. \tag{3.2}$$

Here,

$$\begin{aligned} f_1(x_1, \zeta, y_1) =& a_{200}x_1^2 + a_{101}x_1y_1 + a_{300}x_1^3 + a_{201}x_1^2y_1 + a_{102}x_1y_1^2 \\ &+ O((|x_1| + |\zeta| + |y_1|)^4), \\ g_1(x_1, \zeta, y_1) =& j_{200}x_1^2 + j_{101}x_1y_1 + j_{110}x_1\zeta + j_{011}\zeta y_1 + j_{020}\zeta^2 \\ &+ j_{300}x_1^3 + j_{201}x_1^2y_1 + j_{210}x_1^2\zeta + j_{111}x_1\zeta y_1 + j_{120}x_1\zeta^2 \\ &+ j_{j003}y_1^3 + j_{021}\zeta^2y_1 + j_{030}\zeta^3 + O((|x_1| + |\zeta| + |y_1|)^4) \end{aligned}$$

and

$$\begin{aligned} a_{200} &= -\frac{e^{\frac{2D}{c+D}-d}(AD + Ab - r)}{A}, a_{101} = De^{\frac{2D}{c+D}-d}, \\ a_{300} &= \frac{((b+D)^2A^2 - 2(b+D)rA + r^2 - 2r)e^{\frac{2D}{c+D}-d}}{2A^2} \\ a_{201} &= \frac{De^{\frac{2D}{c+D}-d}((b+D)A - r)}{A}, a_{102} = \frac{D^2e^{\frac{2D}{c+D}-d}}{2} \\ j_{200} &= \frac{D^2}{c+D}, j_{101} = -D, j_{110} = \frac{2D}{c+D}, j_{011} = -1, j_{020} = \frac{1}{c+D}, \end{aligned}$$

$$j_{300} = \frac{D^3}{3(c+D)}, j_{201} = -\frac{D^2}{2}, j_{210} = \frac{D^2}{c+D}, j_{111} = -D,$$

$$j_{120} = \frac{D}{c+D}, j_{003} = \frac{(c+D)^2}{6}, j_{021} = -\frac{1}{2}, j_{030} = \frac{1}{3(c+D)}.$$

Next, we use the following transformation:

$$\begin{pmatrix} x_1 \\ \zeta \\ y_1 \end{pmatrix} = \begin{pmatrix} \frac{(c+D)(e^{\frac{2D}{c+D}-d}+1)}{2D} & 0 & 0 \\ 0 & -c-D & 0 \\ 1 & -1 & 1 \end{pmatrix} \begin{pmatrix} x_2 \\ \tilde{\zeta} \\ y_2 \end{pmatrix}, \tag{3.3}$$

and then get the normal form of (3.1) as follows:

$$\begin{pmatrix} x_2 \\ \tilde{\zeta} \\ y_2 \end{pmatrix} \to \begin{pmatrix} e^{\frac{2D}{c+D}-d} & 0 & 0 \\ 0 & 1 & 0 \\ 0 & 0 & -1 \end{pmatrix} \begin{pmatrix} x_2 \\ \tilde{\zeta} \\ y_2 \end{pmatrix} + \begin{pmatrix} f_2(x_2, \tilde{\zeta}, y_2) \\ 0 \\ g_2(x_2, \tilde{\zeta}, y_2,) \end{pmatrix}, \tag{3.4}$$

where

$$\begin{aligned} f_2(x_2, \tilde{\zeta}, y_2) =& e_{200}x_2^2 + e_{101}x_2y_2 + e_{300}x_2^3 + e_{201}x_2^2y_2 + e_{102}x_2y_2^2 \\ &+ O((|x_2| + |\tilde{\zeta}| + |y_2|)^4), \\ g_2(x_2, \tilde{\zeta}, y_2) =& w_{200}x_2^2 + w_{101}x_2y_2 + w_{110}x_2\tilde{\zeta} + w_{011}\tilde{\zeta}y_2 + w_{020}\tilde{\zeta}^2 + w_{300}x_2^3 \\ &+ w_{201}x_2^2y_2 + w_{210}x_2^2\tilde{\zeta} + w_{102}x_2y_2^2 + w_{111}x_2\tilde{\zeta}y_2 + w_{120}x_2\tilde{\zeta}^2 \\ &+ w_{003}y_2^3 + w_{021}\tilde{\zeta}^2y_2 + w_{030}\tilde{\zeta}^3 + O((|x_2| + |\tilde{\zeta}| + |y_2|)^4) \end{aligned}$$

and

$$\begin{aligned} e_{200} &= -\frac{2De^{\frac{2D}{c+D}-d}(AD + Ab - r)}{A(e^{\frac{2D}{c+D}-d}+1)(c+D)}, \\ e_{101} &= \frac{2D^2e^{\frac{2D}{c+D}-d}}{(e^{\frac{2D}{c+D}-d}+1)(c+D)}, \\ e_{300} &= -\frac{D((b+D)^2A^2 - 2(b+D)rA + r^2 - 2r)e^{\frac{2D}{c+D}-d}}{(e^{\frac{2D}{c+D}-d}+1)(c+D)A^2}, \\ e_{201} &= -\frac{2D^2((b+D)A - r)e^{\frac{2D}{c+D}-d}}{(e^{\frac{2D}{c+D}-d}+1)(c+D)A}, \\ e_{102} &= -\frac{D^3e^{\frac{2D}{c+D}-d}}{(e^{\frac{2D}{c+D}-d}+1)(c+D)}, \end{aligned}$$

$$w_{200} = \frac{2De^{\frac{2D}{c+D}-d}(AD+Ab-r)}{A(e^{\frac{2D}{c+D}-d}+1)(c+D)} + \frac{D^2}{c+D},$$

$$w_{101} = -\frac{2D^2e^{\frac{2D}{c+D}-d}}{(e^{\frac{2D}{c+D}-d}+1)(c+D)} - D,$$

$$w_{110} = -2D, w_{011} = c+D, w_{020} = c+D,$$

$$w_{300} = \frac{D(2r-(bA+DA-r)^2)e^{\frac{2D}{c+D}-d}}{(e^{\frac{2D}{c+D}-d}+1)(c+D)A^2} + \frac{D^3}{3(c+D)},$$

$$w_{201} = \frac{2D^2e^{\frac{2D}{c+D}-d}(bA+DA-r)}{A(e^{\frac{2D}{c+D}-d}+1)(c+D)} - \frac{D^2}{2},$$

$$w_{210} = -D^2, w_{102} = -\frac{D^3e^{\frac{2D}{c+D}-d}}{(e^{\frac{2D}{c+D}-d}+1)(c+D)},$$

$$w_{111} = -D, w_{120} = D(c+D), w_{003} = -\frac{(c+D)^2}{6},$$

$$w_{021} = -\frac{1}{2}, w_{030} = \frac{1}{3}(c+D)^2.$$

By the center manifold theory, the stability of $(x_2, y_2) = (0,0)$ near $\tilde{\zeta} = 0$ can be determined by studying a one-parameter family of reduced equations on a center manifold, which can be represented as follows:

$$W_1^c(0,0,0) = \{(x_2, \tilde{\zeta}, y_2) \in R^3 | x_2 = h(\tilde{\zeta}, y_2), h(0,0) = 0, Dh(0,0) = 0\}.$$

Here, y_2 and $\tilde{\zeta}$ are sufficiently small. We assume that

$$h(\tilde{\zeta}, y_2) = h_1y_2^2 + h_2y_2\tilde{\zeta} + h_3\tilde{\zeta}^2 + O((|\tilde{\zeta}| + |y_2|)^3). \tag{3.5}$$

Then, $h(\tilde{\zeta}, y_2)$ satisfies

$$h(\tilde{\zeta}, -y_2 + g_2(h(\tilde{\zeta}, y_2), \tilde{\zeta}, y_2)) - e^{\frac{2D}{c+D}-d}h(\tilde{\zeta}, y_2) - f_2(h(\tilde{\zeta}, y_2), \tilde{\zeta}, y_2) = 0. \tag{3.6}$$

Substituting (3.5) into (3.6), we obtain

$$h_1 = h_2 = h_3 = 0.$$

Thus, the map on the center manifold is

$$G_1^* : y_2 \to -y_2 + w_{011}\tilde{\zeta}y_2 + w_{020}\tilde{\zeta}^2 + w_{003}y_2^3 + w_{012}\tilde{\zeta}y_2^2 + w_{030}\tilde{\zeta}^3 + O((|\tilde{\zeta}| + |y_2|)^4).$$

A straightforward calculation gives

$$\frac{\partial G_1^*}{\partial y_2}(0,0) = -1, \frac{\partial G_1^*}{\partial \tilde{\zeta}}(0,0) = 0, \frac{\partial^2 G_1^*}{\partial \tilde{\zeta}\partial y_2}(0,0) = w_{011} \neq 0,$$

$$-3(\frac{\partial^2 G_1^*}{\partial y_2^2}(0,0))^2 - 2\frac{\partial^3 G_1^*}{\partial y_2^3}(0,0) = -2w_{003} \neq 0.$$

Therefore, by [24], we can get a flip bifurcation at E_{01}.

In Figure 1(a), we can see that the fixed point $E_{01}(0, \frac{a}{c+D})$ is stable if $0 < a < 2$, and it is unstable if $a > 2$. The maximum Lyapunov exponent is shown in Figure 1(b).

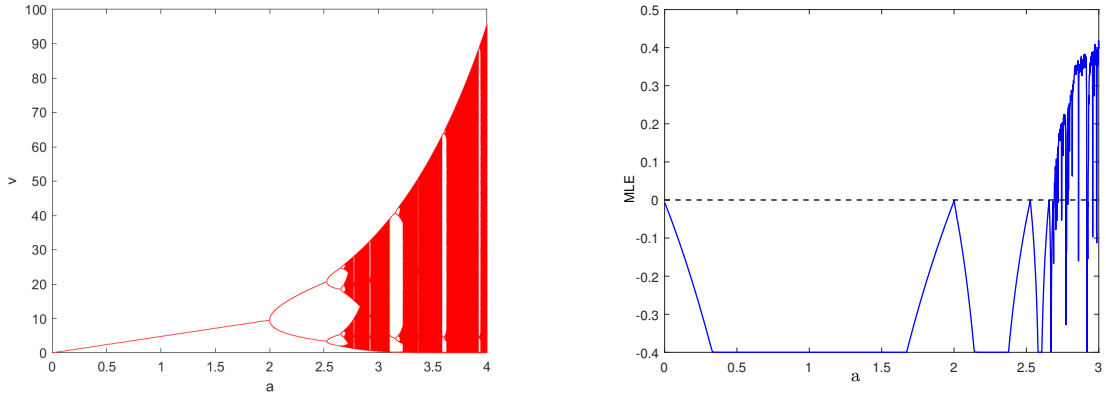

(a) (b)

Figure 1. (a) Bifurcation diagram of $E_{01}(0, \frac{a}{c+D})$, (b) Maximum Lyapunov exponent. We take the parameter values as $a \in [1, 4], D = 0.01, A = 0.01, c = 0.2$ with initial value $(u_0, v_0) = (0.15, 0.2)$.

Theorem 3.2 System (1.4) undergoes a fold bifurcation at $E_{30}(u_3^*, 0)$ if the parameters vary in the small neighborhood of $F_B = \left\{(r, d, D, A) : r > d > 0, D > 0, A = A_1\right\}$.

Proof. From Theorem 2.5, one can have that the eigenvalues of $J(E_{30})$ are $\lambda_1 = 1$ and $\lambda_2 \neq 1, -1$. We choose A as the bifurcation parameter to study fold bifurcation. Let $A = A_1 + \xi$, where ξ is a small perturbation and will be treated as a new variable. System (1.4) is then rewritten as

$$\begin{pmatrix} u \\ v \end{pmatrix} \to \begin{pmatrix} u \exp\left(\dfrac{ru}{(A_1 + \xi) + u} - d - bu + D(v - u)\right) \\ v \exp\left(a - cv + D(u - v)\right) \end{pmatrix}. \tag{3.7}$$

We first use the change of variables $x_3 = u - u_3^*, y_3 = v$ to translate the fixed point $E_{30}(u_3^*, 0)$ to the origin, and then transform system (3.7) into

$$\begin{pmatrix} x_3 \\ \xi \\ y_3 \end{pmatrix} \to \begin{pmatrix} 1 & a_1 & b_1 \\ 0 & 1 & 0 \\ 0 & 0 & e^{a + \frac{D(\sqrt{dr} - d)}{b+D}} \end{pmatrix} \begin{pmatrix} x_3 \\ \xi \\ y_3 \end{pmatrix} + \begin{pmatrix} f_3(x_3, \xi, y_3) \\ 0 \\ g_3(x_3, \xi, y_3) \end{pmatrix}. \tag{3.8}$$

Here,

$$\begin{aligned} f_3(x_3, \xi, y_3) =& b_{200}x_3^2 + b_{110}x_3\xi + b_{101}x_3y_3 + b_{020}\xi^2 + b_{011}\xi y_3 \\ &+ b_{002}y_3^2 + O((|x_3| + |\xi| + |y_3|)^3), \\ g_3(x_3, \xi, y_3) =& z_{002}y_3^2 + z_{101}x_3y_3 + O((|x_3| + |\xi| + |y_3|)^3) \end{aligned}$$

and

$$a_1 = -\frac{r(d-\sqrt{dr})^2}{(r-\sqrt{dr})^2}, b_1 = \frac{rD(\sqrt{dr}-d)(d+r-2\sqrt{dr})}{(D+b)(r-\sqrt{dr})^2},$$

$$b_{200} = \frac{(D+b)r(d\sqrt{dr}+3r\sqrt{dr}-3dr-r^2)(-d+\sqrt{dr})}{(r-\sqrt{dr})^4},$$

$$b_{110} = \frac{8(D+b)r((-\frac{1}{4}d^2-\frac{3}{2}dr-\frac{1}{4}r^2)\sqrt{dr}+dr(d+r))}{(r-\sqrt{dr})^4},$$

$$b_{101} = \frac{((-4d-4r)\sqrt{dr}+d^2+6dr+r^2)Dr^2}{(r-\sqrt{dr})^4},$$

$$b_{020} = \frac{(D+b)r(d-\sqrt{dr})\Big(((-2d+2)r+2d)\sqrt{dr}+dr(d+r-4)\Big)}{2(r-\sqrt{dr})^4},$$

$$b_{011} = \frac{Dr^2((-3d-r)\sqrt{dr}+d(d+3r))(\sqrt{dr}-d)}{(r-\sqrt{dr})^4},$$

$$b_{002} = \frac{D^2r^2(\sqrt{dr}-d)((-4d-4r)\sqrt{dr}+d^2+6dr+r^2)}{2(D+b)(r-\sqrt{dr})^4},$$

$$z_{002} = -(c+D)e^{a+\frac{D(\sqrt{dr}-d)}{b+D}}, z_{101} = De^{a+\frac{D(\sqrt{dr}-d)}{b+D}}.$$

Then, with the transformation,

$$\begin{pmatrix} x_3 \\ \xi \\ y_3 \end{pmatrix} = \begin{pmatrix} 1 & 0 & 1 \\ 0 & -\dfrac{1}{a_1} & 0 \\ 0 & 0 & \dfrac{e^{a+\frac{D(\sqrt{dr}-d)}{b+D}}-1}{b_1} \end{pmatrix} \begin{pmatrix} x_4 \\ \tilde{\xi} \\ y_4 \end{pmatrix}, \tag{3.9}$$

system (3.8) becomes

$$\begin{pmatrix} x_4 \\ \tilde{\xi} \\ y_4 \end{pmatrix} \to \begin{pmatrix} 1 & 1 & 0 \\ 0 & 1 & 0 \\ 0 & 0 & e^{a+\frac{D(\sqrt{dr}-d)}{b+D}} \end{pmatrix} \begin{pmatrix} x_4 \\ \tilde{\xi} \\ y_4 \end{pmatrix} + \begin{pmatrix} f_4(x_4,\tilde{\xi},y_4) \\ 0 \\ g_4(x_4,\tilde{\xi},y_4) \end{pmatrix}, \tag{3.10}$$

where

$$\begin{aligned} f_4(x_4,\tilde{\xi},y_4) =& c_{200}x_4^2 + c_{110}x_4\tilde{\xi} + c_{101}x_4y_4 + c_{020}\tilde{\xi}^2 + c_{011}\tilde{\xi}y_4 \\ &+ c_{002}y_4^2 + O((|x_4|+|\tilde{\xi}|+|y_4|)^3), \\ g_4(x_4,\tilde{\xi},y_4) =& s_{002}y_4^2 + O((|x_4|+|\tilde{\xi}|+|y_4|)^3) \end{aligned}$$

and

$$c_{200} = \frac{(d\sqrt{dr} + 3r\sqrt{dr} - 3dr - r^2)(\sqrt{dr} - d)(D + b)r}{(r - \sqrt{dr})^4},$$

$$c_{110} = \frac{((2r^2 + 12dr + 2d^2)\sqrt{dr} + dr(r + d))(D + b)r}{(r - \sqrt{dr})^4},$$

$$c_{101} = \frac{Dr^2((-4d - 4r)\sqrt{dr} + d^2 + 6dr + r^2)(1 + (b_1 - 1)s)}{(r - \sqrt{dr})^4(s - 1)},$$

$$c_{020} = \frac{\Big(((2 - 2d)r + 2d)\sqrt{dr} + dr(d + r - 4)\Big)r(d - \sqrt{dr})(D + b)}{2(r - \sqrt{dr})^4},$$

$$c_{011} = \frac{((-3d - r)\sqrt{dr} + d(d + 3r))(d - \sqrt{dr})Dr^2}{(r - \sqrt{dr})^4},$$

$$c_{002} = \frac{((-4d - 4r)\sqrt{dr} + d^2 + 6dr + r^2)(d - \sqrt{dr})D^2r^2}{2(D + b)(r - \sqrt{dr})^4} - \frac{b_1 s(D + c)}{s - 1},$$

$$s_{002} = -\frac{b_1 s(D + c)}{s - 1}, s_{101} = \frac{b_1 sD}{s - 1}, s = e^{a + \frac{D(\sqrt{dr} - d)}{b + D}}.$$

According to the central manifold theorem, suppose that an approximate representation of the central manifold $W_2^c(0, 0, 0)$ is as follows:

$$W_2^c(0, 0, 0) = \Big\{(x_4, \tilde{\xi}, y_4) : y_4 = k_1 x_4^2 + k_2 x_4 \tilde{\xi} + k_3 \tilde{\xi}^2 + O((|x_4| + |\tilde{\xi}| + |y_4|)^3)\Big\},$$

where x_4 and $\tilde{\xi}$ are sufficiently small.

By a simple comparison, $k_1 = k_2 = k_3 = 0$ can be obtained. Therefore, the following expression can be easily evaluated:

$$G_2^* : x_4 \to x_4 + \tilde{\xi} + c_{200} x_4^2 + c_{110} x_4 \tilde{\xi} + c_{020} \tilde{\xi}^2 + O((|x_4| + |\tilde{\xi}|)^3).$$

A straightforward calculation gives

$$G_2^*(0, 0) = 0, \frac{\partial G_2^*}{\partial x_4}(0, 0) = 1, \frac{\partial G_2^*}{\partial \tilde{\xi}}(0, 0) = 1, \frac{\partial^2 G_2^*}{\partial x_4^2}(0, 0) = 2c_{200} \neq 0,$$

which leads to the existence of a fold bifurcation.

In Figure 2, the fixed points $E_{10}(u_1^*, 0)$ and $E_{20}(u_2^*, 0)$ bifurcate from $E_{30}(u_3^*, 0)$ when $0 < A < A_1$, coalesce at $E_{30}(u_3^*, 0)$ when $A = A_1$, and disappear when $A > A_1$.

In addition, the fixed points $E_1^*(u_3, v_3)$ and $E_2^*(u_3, v_3)$ bifurcate from $E_3^*(u_3, v_3)$ when $m < m_1$, merge at $E_3^*(u_3, v_3)$ when $m = m_1$, and vanish when $m > m_1$. Thus, we can have the existence of a fold bifurcation as follows:

Theorem 3.3 When $d^{**} < d < d^{**} + r$ and $m = m_1$, system (1.4) undergoes a fold bifurcation at $E_3^*(u_3, v_3)$.

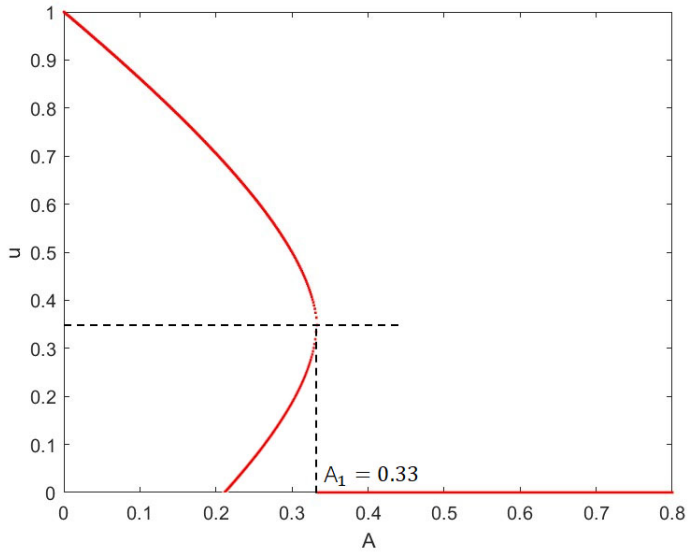

Figure 2. Fold bifurcation diagram of $E_{30}(u_3^*, 0)$. We take the parameter values as $d = 0.3, b = 0.3, D = 0.6, r = 1.2$, and with initial value $(u_0, v_0) = (0.5, 0.6)$.

Proof. Denote

$$F_C = \Big\{(r, d, m) : r > 0, d^{**} < d < d^{**} + r, m = m_1\Big\}.$$

Since $m = b + \frac{cD}{c+D}$, we choose b as a bifurcation parameter for studying the fold bifurcation of $E_3^*(u_3, v_3)$. Let $b = b^* + \delta$, where $b^* = m - \frac{cD}{c+D}$. δ is a small perturbation and will be treated as a new variable. System (1.4) is then rewritten as

$$\begin{pmatrix} u \\ v \end{pmatrix} \to \begin{pmatrix} u\exp(\dfrac{ru}{A+u} - d - (b^* + \delta)u + D(v-u)) \\ v\exp\left(a - cv + D(u-v)\right) \end{pmatrix}. \tag{3.11}$$

The eigenvalues of $J_{E_3^*}$ are $\lambda_1 = 1, \lambda_2 \neq 1$ by Theorem 2.7. We first use the change of variables $x_5 = u - u_3, y_5 = v - v_3$ to translate the positive fixed point $E_3^*(u_3, v_3)$ to the origin and then transform system (1.4) into

$$\begin{pmatrix} x_5 \\ y_5 \end{pmatrix} \to \begin{pmatrix} p_{11} & p_{12} \\ p_{21} & p_{22} \end{pmatrix} \begin{pmatrix} x_5 \\ y_5 \end{pmatrix} + \begin{pmatrix} f_5(x_5, \delta, y_5) \\ g_5(x_5, \delta, y_5) \end{pmatrix}. \tag{3.12}$$

Here,

$$\begin{aligned} f_5(x_5, \delta, y_5) =& p_{200}x_5^2 + p_{110}x_5\delta + p_{101}x_5y_5 + p_{020}\delta^2 + p_{011}\delta y_5 \\ &+ p_{002}y_5^2 - u_3^2\delta + O((|x_5| + |\delta| + |y_5|)^3), \\ g_5(x_5, \delta, y_5) =& q_{200}x_5^2 + q_{002}y_5^2 + q_{101}x_5y_5 + O((|x_5| + |\delta| + |y_5|)^3) \end{aligned}$$

and

$$p_{11} = \frac{1}{(A+u_3)^2}((Dv_3 - d + r - 1)u_3^2 + 2A(Dv_3 - d - 1)u_3$$

$$
\begin{aligned}
&+ (Dv_3 - d - 1)A^2),\\
p_{12} =& u_3 D, \quad p_{21} = v_3 D, \quad p_{22} = Dv_3 - cv_3 - 2,\\
p_{200} =& \frac{1}{2u_3(A+u_3)^4}((Dv_3 - d + r - 2)(Dv_3 - d + r)u_3^4\\
&+ 4A(D^2 v_3^2 - 2(d - \frac{r}{2} + 1)Dv_3 + d^2 + (2 - r)d - \frac{3r}{2}u_3^3\\
&+ 6(Dv_3 - d + \frac{r}{3})A^2(Dv_3 - d - 2)u_3^2 + 4A^3(Dv_3 - d - 2)(Dv_3 - d)u_3\\
&+ A^4(Dv_3 - d - 2)(Dv_3 - d)),\\
p_{110} =& \frac{u_3}{(A+u_3)^2}((Dv_3 - d + r - 2)u_3^2 + 2A(Dv_3 - d - 2)u_3 + (Dv_3 - d - 2)A^2),\\
p_{101} =& -\frac{D((D + b^*)u_3^3 + (2DA + 2bA - 1)u_3^2 + (DA + b^*A - r - 2)Au_3 - A^2)}{(A+u_3)^2},\\
p_{020} =& \frac{u_3^3}{2}, p_{011} = -u_3^2 D, \quad p_{002} = \frac{u_3 D^2}{2},\\
q_{200} =& \frac{v_3 D^2}{2}, \quad q_{101} = D(1 - Dv_3 + cv_3), \quad q_{002} = \frac{(c+D)(Dv_3 + cv_3 - 2)}{2}.
\end{aligned}
$$

We construct an invertible matrix

$$
\mathrm{T} = \begin{pmatrix} p_{12} & p_{12} \\ 1 - p_{11} & \lambda_2 - p_{11} \end{pmatrix}
$$

and use the translation

$$
\begin{pmatrix} x_5 \\ y_5 \end{pmatrix} = \mathrm{T} \begin{pmatrix} x_6 \\ y_6 \end{pmatrix},
$$

and then the map (3.12) becomes

$$
\begin{pmatrix} x_6 \\ y_6 \end{pmatrix} = \begin{pmatrix} 1 & 0 \\ 0 & \lambda_2 \end{pmatrix} \begin{pmatrix} x_6 \\ y_6 \end{pmatrix} + \begin{pmatrix} f_6(x_6, \tilde{\delta}, y_6) \\ g_6(x_6, \tilde{\delta}, y_6) \end{pmatrix}, \tag{3.13}
$$

where

$$
\begin{aligned}
f_6(x_6, \tilde{\delta}, y_6) =& \frac{(\lambda_2 - p_{11})p_{200} - u_3 D q_{200}}{u_3 D(\lambda_2 - 1)} x_5^2 + \frac{(\lambda_2 - p_{11})q_{101}}{u_3 D(\lambda_2 - 1)} x_5 \tilde{\delta}\\
&+ \frac{(\lambda_2 - p_{11})p_{101} - u_3 D q_{101}}{u_3 D(\lambda_2 - 1)} x_5 y_5 + \frac{(\lambda_2 - p_{11})p_{020}}{u_3 D(\lambda_2 - 1)} \tilde{\delta}^2\\
&+ \frac{(\lambda_2 - p_{11})p_{011}}{u_3 D(\lambda_2 - 1)} \tilde{\delta} y_5 + \frac{(\lambda_2 - p_{11})p_{002} - u_3 D q_{002}}{u_3 D(\lambda_2 - 1)} y_5^2\\
&- \frac{(\lambda_2 - p_{11})u_3^2 \delta}{u_3 D(\lambda_2 - 1)} + O((|x_5| + |\tilde{\delta}| + |y_5|)^3),
\end{aligned}
$$

$$
\begin{aligned}
g_6(x_6,\tilde{\delta},y_6) =& \frac{(1-p_{11})p_{200}+u_3Dq_{200}}{u_3D(\lambda_2-1)}x_5^2+\frac{(1-p_{11})p_{002}+u_3Dq_{002}}{u_3D(\lambda_2-1)}y_5^2\\
&+\frac{(1-p_{11})p_{101}+u_3Dq_{101}}{u_3D(\lambda_2-1)}x_5y_5+\frac{(1-p_{11})p_{110}}{u_3D(\lambda_2-1)}x_5\delta\\
&+\frac{(1-p_{11})p_{020}}{u_3D(\lambda_2-1)}\delta^2+\frac{(1-p_{11})p_{011}}{u_3D(\lambda_2-1)}\delta y_5\\
&-\frac{(1-p_{11})u_3^2}{u_3D(\lambda_2-1)}\delta+O((|x_5|+|\tilde{\delta}|+|y_5|)^3)
\end{aligned}
$$

and

$$
\begin{aligned}
x_5 &= u_3Dx_6+u_3Dy_6,\\
y_5 &= (1-p_{11})x_6+(\lambda_2-p_{11})y_6,\\
x_5^2 &= u_3^2D^2(x_6^2+2x_6y_6+y_6^2),\\
y_5^2 &= (1-p_{11})^2x_6^2+(\lambda_2-p_{11})^2y_6^2+2(1-p_{11})(\lambda_2-p_{11})x_6y_6,\\
x_5y_5 &= (1-p_{11})u_3Dx_6^2+u_3D(1-2p_{11}+\lambda_2)x_6y_6+u_3D(\lambda_2-p_{11})y_6^2.
\end{aligned}
$$

Next, an approximate representation of the central manifold $W_3^c(0,0,0)$ is supposed as follows:

$$
W_3^c(0,0,0)=\left\{(x_6,\tilde{\delta},y_6):y_6=t_1x_6^2+t_2x_6\tilde{\delta}+t_3\tilde{\delta}^2+O((|x_6|+|\tilde{\delta}|+|y_6|)^3)\right\},
$$

where

$$
\begin{aligned}
t_1 =& \frac{p_{11}-1}{(1-\lambda_2)^2}[(1-p_{11})(p_{101}+q_{002})+u_3D(p_{200}+q_{101})\\
&+\frac{D(1-p_{11})}{2}]-\frac{u_3^3D^2q_{200}}{(1-\lambda_2)^2},\\
t_2 =& \frac{Dp_{110}(p_{11}-1)}{u_3(1-\lambda_2)(\lambda_2-p_{11})}+\frac{D(1-p_{11})^2}{(1-\lambda_2)(\lambda_2-p_{11})},\\
t_3 =& \frac{D(p_{11}-1)}{2(p_{11}-\lambda_2)^2}.
\end{aligned}
$$

Therefore, we consider the map restricted to the center manifold $W_3^c(0,0,0)$:

$$
G_3^*: x_6\to x_6+\tilde{\delta}+n_1x_6^2+n_2x_6\tilde{\delta}+n_3\tilde{\delta}^2+n_4x_6^3+n_5x_6^2\tilde{\delta}+O((|x_6|+|\tilde{\delta}|)^4).
$$

Here,

$$
\begin{aligned}
n_1 =& \frac{1}{\lambda_2-1}\{(\lambda_2-p_{11})[p_{200}+p_{101}(1-p_{11})+\frac{D(1-p_{11})^2}{2}]\\
&+(p_{11}-1)(u_3Dq_{101}-q_{002}p_{11}+q_{002})-u_3Dq_{200}\},\\
n_2 =& D-Dp_{11}-\frac{Dq_{101}}{u_3},\quad n_3=\frac{D(\lambda_2-1)p_{020}}{u_3^2(\lambda_2-p_{11})},
\end{aligned}
$$

$$
\begin{aligned}
n_4 =& \frac{t_1}{\lambda_2 - 1}[2u_3 D p_{200}(\lambda_2 - p_{11}) - 2u_3^2 D^2 q_{200} \\
&+ (\lambda_2 p_{101} - p_{11} p_{101} - u_3 D q_{101})(1 - 2p_{11} + \lambda_2) \\
&+ D(\lambda_2 - p_{11})^2(1 - p_{11}) - 2q_{002}(1 - p_{11})(\lambda_2 - p_{11})], \\
n_5 =& \frac{t_2}{\lambda_2 - 1}[2u_3 D p_{200}(\lambda_2 - p_{11}) - 2u_3^2 D^2 q_{200} \\
&+ (\lambda_2 p_{101} - p_{11} p_{101} - u_3 D q_{101})(1 - 2p_{11} + \lambda_2) + D(\lambda_2 - p_{11})^2(1 - p_{11}) \\
&- 2q_{002}(1 - p_{11})(\lambda_2 - p_{11})] + (\lambda_2 D - p_{11} D - \frac{D q_{101}}{u_3}) t_1, \\
n_6 =& \frac{t_3}{\lambda_2 - 1}[2u_3 D p_{200}(\lambda_2 - p_{11}) - 2u_3^2 D^2 q_{200} \\
&+ (\lambda_2 p_{101} - p_{11} p_{101} - u_3 D q_{101})(1 - 2p_{11} + \lambda_2) + D(\lambda_2 - p_{11})^2(1 - p_{11}) \\
&- 2q_{002}(1 - p_{11})(\lambda_2 - p_{11})] + (\lambda_2 D - p_{11} D - \frac{D q_{101}}{u_3}) t_2, \\
n_7 =& (\lambda_2 D - p_{11} D - \frac{D q_{101}}{u_3}) t_3.
\end{aligned}
$$

A straightforward calculation gives

$$
G_3^*(0,0) = 0,\ \frac{\partial G_3^*}{\partial x_6}(0,0) = 1,\ \frac{\partial G_3^*}{\partial \delta}(0,0) = 1,\ \frac{\partial^2 G_3^*}{\partial x_6^2}(0,0) = 2n_1,
$$

which leads to the existence of a fold bifurcation.

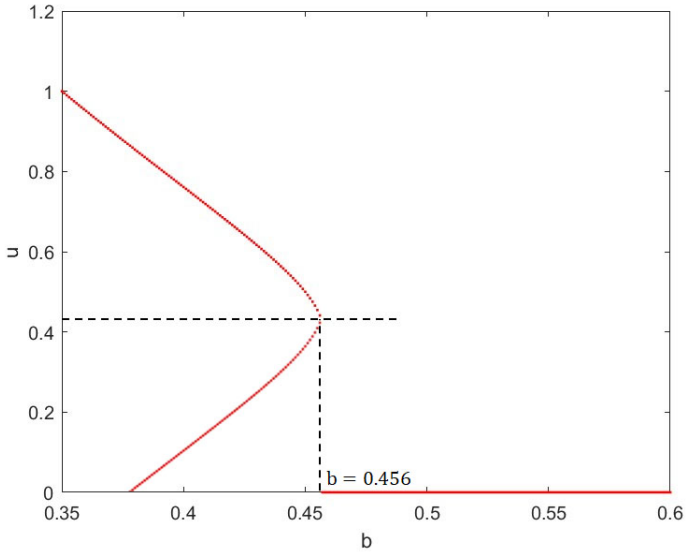

Figure 3. Fold bifurcation diagram of $E_3^*(u_3, v_3)$ with respect to the parameter b when $d = 0.7, A = 1, D = 0.6, r = 1.2, a = 0.8, c = 0.2$, $b \in (0.35, 0.6)$, and the initial point is $(0.7, 0.6)$.

In Figure 3, the parameter values are $d = 0.7, A = 1, D = 0.6, r = 1.2, a = 0.8, c = 0.2$, and the initial value is $(u_0, v_0) = (0.7, 0.6)$. We have $b = 0.456$ and calculate $u_3 = 0.436$ from Theorem 2.2. In other words, the positive fixed points $E_1^*(u_1, v_1)$ and $E_2^*(u_2, v_2)$ bifurcate from $E_3^*(u_3, v_3)$ when $0.38 < b < 0.456$, merge at $E_3^*(u_3, v_3)$ when $b = 0.456$, and vanish when $b > 0.456$.

4. Effect of the Allee effect and nonlinear dispersal

In this section, we will explore the impact of the Allee effect and nonlinear dispersal on population survival through numerical simulations. As is well known, when population density is low, the Allee effect can lead to a decrease in cooperation and mutual assistance among individuals, thereby reducing the growth rate of the population. We choose

$$(a, r, c, D, b, d) = (1.5, 1.2, 0.2, 0.1, 0.3, 0.4)$$

and the initial values of the system (1.4) are $(0.7, 0.2)$ and $(0.5, 0.4)$. As is shown in Figure 4, when the Allee constant $A = 0$, the population density u is relatively high and oscillates greatly. When the Allee constant $A = 0.5$ or $A = 1.5$, the population density decreases and oscillations become less frequent. Increasing Allee effect can effectively reduce the oscillation amplitude of the solution. In this sense, the Allee effect has a stabilizing ability.

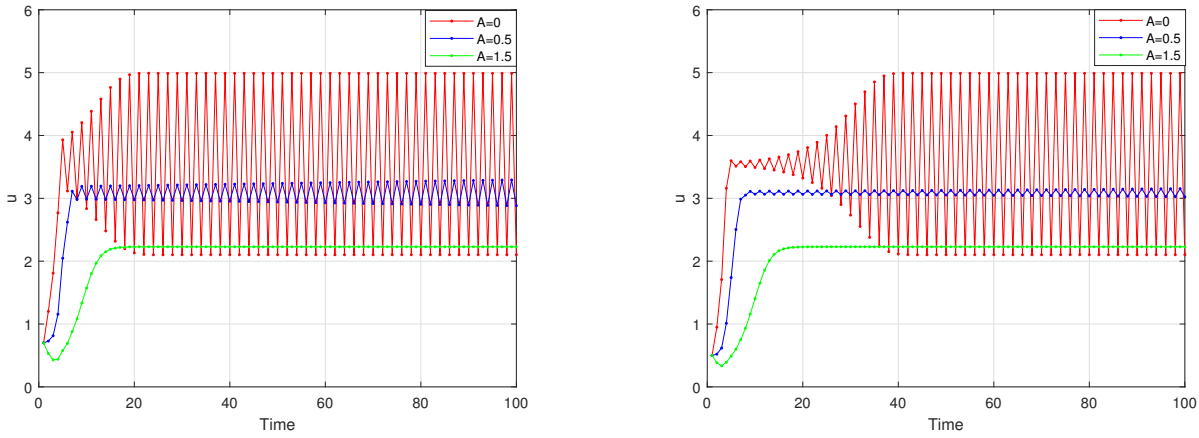

(a) The initial value is $(0.7, 0.2)$.

(b) The initial value is $(0.5, 0.4)$.

Figure 4. The oscillation of system (1.4) when $a = 1.5, r = 1.2, c = 0.2, D = 0.1, b = 0.3, d = 0.4$, and the initial points are $(0.7, 0.2)$, $(0.5, 0.4)$.

In Figure 5, we take $(a, r, c, A, b, d) = (1.5, 1.2, 0.2, 3, 0.3, 0.4)$ and initial values $(0.7, 0.2)$ and $(0.5, 0.4)$. It follows that when the dispersal coefficient $D = 0$, population u goes extinct while population v is permanent. When $D = 0.1$, both populations coexist. As the dispersal coefficient keeps increasing, the fluctuations of both populations become significant. Figure 5 shows that when there is no nonlinear dispersal, the population will tend to be extinct due to the Allee effect. Moreover, large nonlinear dispersal will also lead to fluctuations of the population. That is to say, proper proliferation is conducive to population survival.

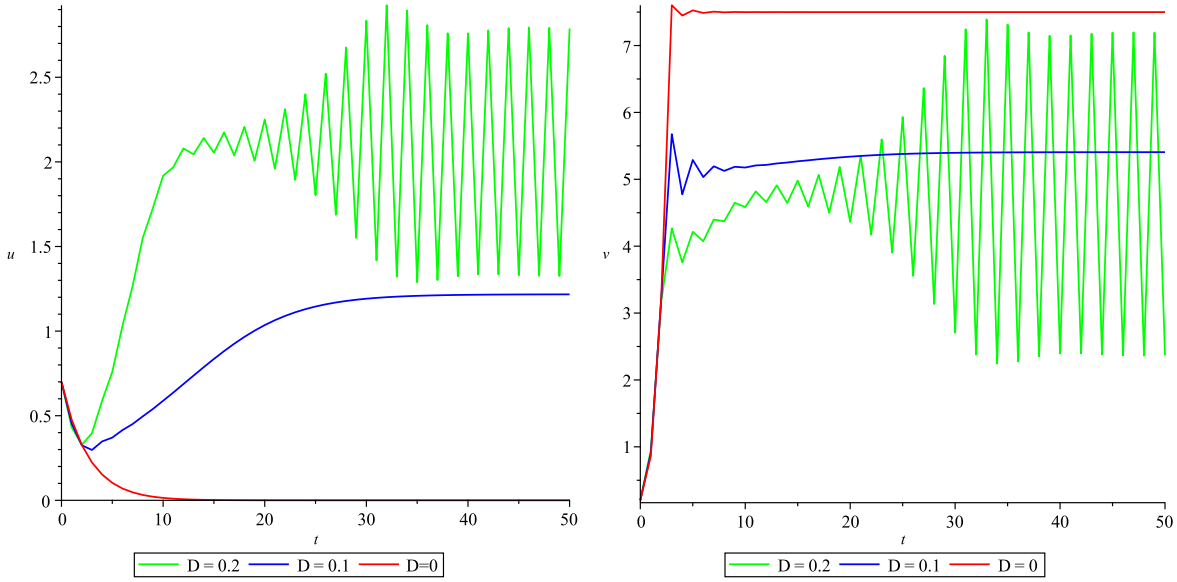

(a) The initial value is $(0.7, 0.2)$.

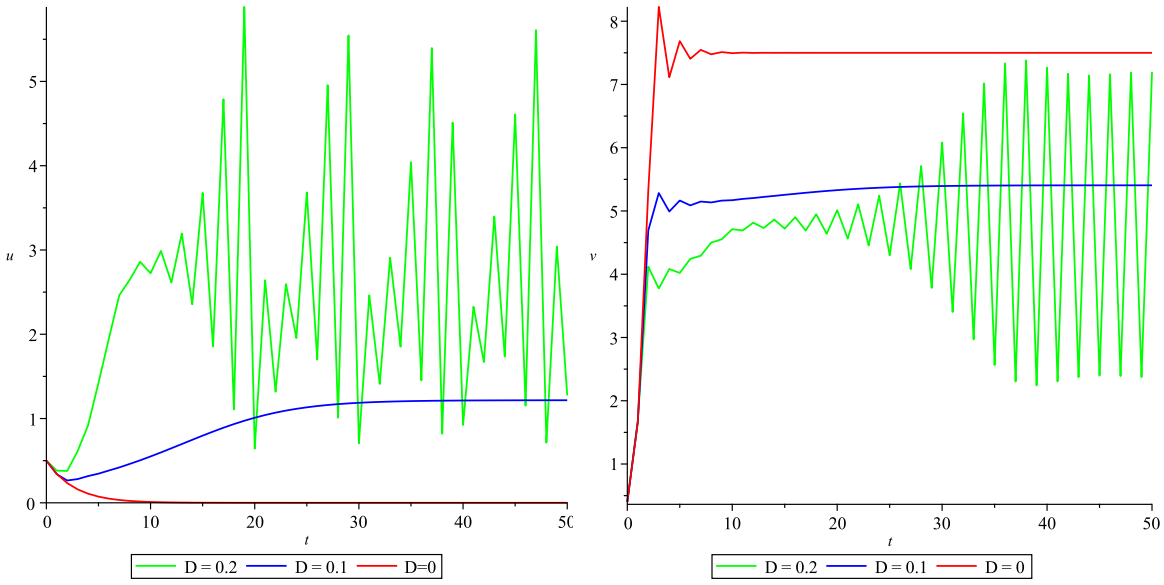

(b) The initial value is $(0.5, 0.4)$.

Figure 5. Time series of system (1.4) under different dispersal when $a = 1.5, r = 1.2, c = 0.2, A = 3, b = 0.3, d = 0.4$, and the initial points are $(0.7, 0.2)$, $(0.5, 0.4)$.

5. Summary

In this paper, we have considered a discrete two-patch model with Allee effect and nonlinear dispersal based on Xia et al. [14]. The dynamic behaviors have been analyzed in detail. We discuss the existence of fixed points, the flip bifurcation at the boundary fixed point $E_{01}(0, \frac{a}{c+D})$, the fold bifurcation at the boundary fixed point $E_{30}(u_3^*, 0)$, and the positive fixed point $E_3^*(u_3, v_3)$, respectively. The impact of the Allee effect and nonlinear dispersal on population survival is also presented through numerical simulation.

The topological types of the fixed points are substantially different from those in Xia et al. [14] and Grumbach et al. [17]. In detail, the model in this manuscript has a maximum of two positive fixed points, whereas the similar discrete model in [17] has a unique positive fixed point. Moreover, the discrete model can experience a flip bifurcation at the boundary fixed point E_{01} when the conditions $a = 2, a \neq \frac{d(c+D)}{D}$ hold, while the corresponding boundary equilibrium E_v in the continuous model [14] is globally asymptotically stable under certain conditions. In addition, the results in Xia et al. [14] show that for the continuous case, large nonlinear dispersal may prevent the extinction of species due to the Allee effect. But in this paper, we obtain that small or high nonlinear dispersal will lead to extinction or fluctuations, and only moderate and appropriate nonlinear dispersal can make the species become permanent. In other words, suitable and modest dispersal is advantageous to the survival of the species. The aforementioned point is due to the fact that modest dispersal minimizes intense rivalry with others for resources like food, habitat, and breeding space. But, when the dispersal coefficient is large, the species will go extinct because dispersal increases the complexity of the system, and makes it more susceptible to external influence. Therefore, the conclusion of this article is a complement and promotion of [14] and [17].

Use of AI tools declaration

The authors declare they have not used Artificial Intelligence (AI) tools in the creation of this article.

Acknowledgments

This work was supported by the National Natural Science Foundation of China under Grant (11601085) and the Natural Science Foundation of Fujian Province (2021J01614, 2021J01613).

Conflict of interest

The authors declare there is no conflict of interest.

References

1. W. Allee, *Animal Aggregations: A Study in General Sociology*, University of Chicago Press, Chicago, 1931.
2. T. Liu, L. Chen, F. Chen, Z. Li, Stability analysis of a Leslie–Gower model with strong Allee effect on prey and fear effect on predator, *Int. J. Bifurcation Chaos*, **32** (2022), 2250082. https://doi.org/10.1142/S0218127422500821
3. T. Liu, L. Chen, F. Chen, Z. Li, Dynamics of a Leslie–Gower model with weak Allee effect on prey and fear effect on predator, *Int. J. Bifurcation Chaos*, **33** (2023), 2350008. https://doi.org/10.1142/S0218127423500086
4. C. Çelik, O. Duman, Allee effect in a discrete-time predator–prey system, *Chaos, Solitons Fractals*, **40** (2009), 1956–1962. https://doi.org/10.1016/j.chaos.2007.09.077
5. S. Saha, G. Samanta, Influence of dispersal and strong Allee effect on a two-patch predator–prey model, *Int. J. Dyn. Control*, **7** (2019), 1321–1349. http://doi.org/10.1007/s40435-018-0490-3

6. Y. Kang, S. Kumar Sasmal, K. Messan, A two-patch prey-predator model with predator dispersal driven by the predation strength, *Math. Biosci. Eng.*, **14** (2017), 843–880. http://doi.org/10.3934/mbe.2017046
7. W. Wang, Population dispersal and Allee effect, *Ric. Mat.*, **65** (2016), 535–548. https://doi.org/10.1007/s11587-016-0273-0
8. D. Pal, G. Samanta, Effects of dispersal speed and strong Allee effect on stability of a two-patch predator–prey model, *Int. J. Dyn. Control*, **6** (2018), 1484–1495. https://doi.org/10.1007/s40435-018-0407-1
9. Y. Kang, N. Lanchier, Expansion or extinction: deterministic and stochastic two-patch models with Allee effects, *J. Math. Biol.*, **62** (2011), 925–973. https://doi.org/10.1007/s00285-010-0359-3
10. L. Chen, T. Liu, F. Chen, Stability and bifurcation in a two-patch model with additive Allee effect, *AIMS Math.*, **7** (2022), 536–551. http://doi.org/10.3934/math.2022034
11. L. Allen, Persistence and extinction in single-species reaction-diffusion models, *Bull. Math. Biol.*, **45** (1983), 209–227. https://doi.org/10.1016/S0092-8240(83)80052-4
12. X. Zhang, L. Chen, The linear and nonlinear diffusion of the competitive Lotka–Volterra model, *Nonlinear Anal. Theory Methods Appl.*, **66** (2007), 2767–2776. https://doi.org/10.1016/j.na.2006.04.0068
13. X. Zhou, X. Shi, X. Song, Analysis of nonautonomous predator-prey model with nonlinear diffusion and time delay, *Appl. Math. Comput.*, **196** (2008), 129–136. https://doi.org/10.1016/j.amc.2007.05.041
14. Y. Xia, L. Chen, V. Srivastava, R. Parshad, Stability and bifurcation analysis of a two-patch model with Allee effect and nonlinear dispersal, *Math. Biosci. Eng.*, **20** (2023), 19781–19807. https://doi.org/10.48550/arXiv.2310.10558
15. J. Chen, Y. Chen, Z. Zhu, F. Chen, Stability and bifurcation of a discrete predator-prey system with Allee effect and other food resource for the predators, *J. Appl. Math. Comput.*, **69** (2023), 529–548. https://doi.org/10.1007/s12190-022-01764-5
16. Q. Zhou, Y. Chen, S. Chen, F. Chen, Dynamic analysis of a discrete amensalism model with Allee effect, *J. Appl. Anal. Comput.*, **13** (2023), 2416–2432. https://doi.org/10.11948/20220332
17. C. Grumbach, F. Reurik, J. Segura, F. Hilker, The effect of dispersal on asymptotic total population size in discrete-and continuous-time two-patch models, *J. Math. Biol.*, **87** (2023), 60. https://doi.org/10.1007/s00285-023-01984-8
18. C. Guiver, D. Packman, S. Townley, A necessary condition for dispersal driven growth of populations with discrete patch dynamics, *J. Theor. Biol.*, **424** (2017), 11–25. https://doi.org/10.1016/j.jtbi.2017.03.030
19. H. Jiang, T. Rogers, The discrete dynamics of symmetric competition in the plane, *J. Math. Biol.*, **25** (1987), 573–596. https://doi.org/10.1007/BF00275495
20. X. Liu, D. Xiao, Complex dynamic behaviors of a discrete-time predator-prey system, *Chaos, Solitons Fractals*, **32** (2007), 80–94. https://doi.org/10.1016/j.chaos.2005.10.081
21. J. Chen, X. He, F. Chen, The influence of fear effect to a discrete-time predator-prey system with predator has other food resource, *Mathematics*, **9** (2021), 865. https://doi.org/10.3390/math9080865

22. J. Guckenheimer, P. Holmes, *Nonlinear Oscillations, Dynamical Systems, and Bifurcations of Vector Fields*, Springer Science & Business Media, **42** (2013).

23. C. Robinson, *Dynamical Systems: Stability, Symbolic Dynamics and Chaos*, CRC Press, Boca Raton, 1998.

24. Y. Kuznetsov, *Elements of Applied Bifurcation Theory*, Springer, New York, **112** (1998). https://doi.org/10.1007/978-1-4757-3978-7

AIMS Press